Agent Simulation Using Path Telemetry for Modeling COVID-19 Workplace Hazard and Risk

David Beymer[1], Vandana Mukherjee[1], Anup Pillai[1], Hakan Bulu[1], Vanessa Burrowes[2], James Kaufman[1,*] and Ed Seabolt[1]

[1]*IBM Research - Almaden, 650 Harry Rd, San Jose, CA 95120, U.S.A.*

[2]*IBM, 3039 E Cornwallis Rd, Research Triangle Park, NC 27709, U.S.A.*

Keywords: Computer Simulation, Agent-Based Modeling, Epidemiological Modeling, Risk Analysis, Safety Management.

Abstract: We present a cloud native agent based simulation of disease transmission hazard and risk in a model of a particular workplace. When combined with epidemiological data for employee home counties, the simulation can be used to measure the effect of interventions and building policies on occupational hazard and risk from an infectious disease, and to compare that hazard and risk to the average risk to the employees in their home counties based on current outbreak data. We demonstrate this for two particular interventions, varying the number of employees allowed to work onsite, and enabling/disabling alternate routes at choke points such as cafeteria checkpoints. We discuss how occupational hazard and risk depends strongly on the details of workplace layout and policies and propose how the current simulation (and tools like it) can be used to evaluate policies and procedures for return to work.

1 INTRODUCTION

The pandemic disease COVID-19, caused by the SARS-CoV-2 virus, disrupted economies and lifestyles worldwide. As new variants continued to evolve and emerge, many organizations struggled to develop consistent and robust guidelines for policies that supported a ”safe” return to work. The process is confounded as the rates of viral transmission change with the evolution of the virus as it adapts to human host populations as well as to the changing landscape of host immunity.

Understanding which policies might best support a ”safe” return to work first requires an agreed definition of safety, along with quantitative measures for both hazard and risk (Hosseini et al., 2017; Kumpulainen, 2006; Sage and White, 1980). Assessment of occupational risk requires quantification of the potential hazards a person encounters in a workplace environment (Daniels et al., 2020). No workplace is completely free of risk, but in the context of infectious disease exposure one might classify a workplace as ”safe” if the exposure hazard and disease transmission risk are less than the corresponding hazards and risks an individual might face in the same time span had they not come to the workplace. This baseline risk depends, of course, on interventions, policies, and practices in their jurisdiction of residence, but the data required to measure local hazard and risk is currently available in most jurisdictions through local public health reporting. In this paper we apply epidemiological compartment modeling (Gopalakrishnan et al., 2021b; Gopalakrishnan et al., 2021a; Baldassi et al., 2021; Douglas et al., 2019; Bianco et al., 2021) to the home counties of employees in a simulated workforce to drive an agent based simulation of a real workplace.

Agent-based models, which have been used in a variety of fields such as economics, business, gaming and the social sciences, construct a simulated environment of independent agents, from whose simple rules of interaction an emergent system behavior arises. Agent based modeling has been used to study how workplace policies and practices influence workplace outcomes across a variety of dimensions (Muñoz and Iglesias, 2021; Duggirala et al., 2016; Hardy et al., 2021; Vitins et al., 2016). Some agent-based systems have included strong spatial support, such as the use of GIS concepts in the GAMA platform (Tail-

*J. Kaufman is currently with Altos Labs, Bay Area Institute of Science, 1300 Island Drive, Redwood City, CA 94065, U.S.A.

Beymer, D., Mukherjee, V., Pillai, A., Bulu, H., Burrowes, V., Kaufman, J. and Seabolt, E.
Agent Simulation Using Path Telemetry for Modeling COVID-19 Workplace Hazard and Risk.
DOI: 10.5220/0012322400003657

In *Proceedings of the 17th International Joint Conference on Biomedical Engineering Systems and Technologies (BIOSTEC 2024) - Volume 1*, pages 417-428
ISBN: 978-989-758-688-0; ISSN: 2184-4305

landier et al., 2018), and social simulations built on top (BEN system (Bourgais et al., 2019)). When applied to epidemiology, the agent-based model allows for social networks between the agents to be studied for their impact on viral dynamics. In (Kerr et al., 2021; Hinch et al., 2021; Chang et al., 2020), agent networks are formed consisting of households, schools, workplaces, and random connections for interactions with the community-at-large. An epidemiological model is placed over the agents, and the effects of different simulated COVID-19 interventions such as masks, contact tracing, or quarantine can be studied. With the agent network, one could model, for instance, how a virus can be transmitted from a school to a workplace via child-to-parent infection in a household. The OpenCOVID (Shattock et al., 2022) agent simulation system constructs an agent network based on the observation that the number of agent contacts per day is age-dependent, peaking in middle age. Transmission between agents takes into consideration the viral load of the infectious agent, the infectivity factor of the COVID variant, a seasonality factor, and the immunity of the susceptible agent.

In existing agent-based systems, the spatial location of agents is typically modeled at a very coarse level, such as presence in a household, school, or workplace. Infection within a specific location is handled by assuming that each agent has a certain number of contacts, and then these contacts are randomly chosen from the agents present. One exception is (Islam et al., 2022), where, similar to our work, they model the detailed movement of agents in a plan map. Instead of COVID in the workplace, they focus on modeling student agents in an campus setting, evaluating the placement of classroom seating to mitigate the spread of COVID.

In the context of infectious disease work, we define workplace hazard as the cumulative contact time between all pairs of people. Contact is defined in terms of a configurable hazard radius. Risk is then the pairwise transmission risk, as defined by mathematical epidemiology. Actual county level public health data determines the average disease burden (as a function of time) in the employees home county, and epidemiological modeling is used to measure transmission rates and other epidemiological parameters based on these data. These parameters reflect the time varying policies and practices in each home county. With this framework it is possible to compare the expected hazard and risk any employee might face in any particular workday to the population based hazard and risk measured for each home county. Furthermore, the agent based simulation supports a quantitative assessment of workplace practices put in place to reduce occupational hazard and risk from SARS-CoV-2.

We present an agent-based simulation system that estimates COVID-19 hazard and risk by recording pairwise interactions between simulated employee agents in the workplace. Simulated agents move about a plan map view of the workplace, guided by a calendaring service that sets the daily schedule for each agent, which includes meetings, lunch, and coffee and restroom breaks. The natural office work structure is re-created by placing agents in a virtual organizational chart. Agents in the same organizational line have assigned offices next to one another and will have scheduled meetings with one another. As agents move about the workplace, our system records hazard and risk when agents are within a distance threshold. Epidemiological compartmental modeling is used to seed some agents as infected, using transmission rates from their home county, and then the workday simulation will record exposure events to other susceptible agents.

Comparing our proposed system to existing agent-based systems, the former tend to operate at a macro level, modeling entire countries or metropolitan regions (Kerr et al., 2021; Hinch et al., 2021; Shattock et al., 2022). The location of agents and their interactions happens at an abstract level, in census block groups (Chang et al., 2021), statistical local areas (Chang et al., 2020) or even more abstracted as ”school” or ”workplace”. We focus on a particular workplace site, adding a floor plan map and modeling detailed (x, y) telemetry of agents in the floor plan. This allows our system to model specific virus transmission events at an exact location between the infected and susceptible agents. We don't need to postulate, as in the more generic agent-based approach, general exposure risks when two agents are in the same generic context like a school or household. Secondly, for interventions, this allows the exploration of how modifications to the floor plan changes agents' behavior and hence infection events. And finally, for reporting, our system allows for visualizations based on the floor plan, such as heat maps of exposure events in the building. This reveals trouble spots in the floor plan that may require tweaking to improve agent / employee traffic flow.

In this paper, we use the agent-based simulation system to quantitatively compare COVID-19 hazard and risk for different workplace policies or interventions. By plotting this risk as a function of building occupancy, we can look for intersection points with the same risk curve of the same agents working from home. This crossover point suggests a safe operation building occupancy, where workplace risk equals the county-based working-from-home rate. We perform

this analysis for two building policies and also look at the effect that vaccinations have on the process.

2 METHODS

2.1 Epidemiology

2.1.1 Epidemiological Data

This study uses data from the USAFacts COVID-19 datasets (USAFacts, 2020) to measure the baseline, time varying, disease hazard and risk in each employees home county. This data includes daily COVID-19 confirmed cases and deaths, compiled by the CDC, and obtained directly from state and local agencies. For the two building interventions tested in detail, all agent based simulation runs were done for a full workday on the date July 30, 2021. Later, for a historical analysis, the date range is opened up to a series of dates in 2021 and 2022; in principle, any series of dates can be chosen. Where historic data exists, county disease prevalence is taken from the historic data. For a chosen 1-4 weeks into the future, county disease prevalence would be predicted by epidemiological modeling.

2.1.2 Epidemiological Model

To derive the time varying epidemiological parameters from this data, we chose the SpatioTemporal Epidemiological Modeler (STEM) (Douglas et al., 2019; Edlund et al., 2010), a modeling framework available through the Eclipse Foundation (Kaufman, 2022). The framework and model are open source and available under the Eclipse Public License (EPL2) (Alamoudi et al., 2020). STEM supports a variety of models and provides a graphical model design tool for new model composition (Baldassi et al., 2021). The particular model used in this study, the compartmental model, is discussed in detail elsewhere (Gopalakrishnan et al., 2021b; Gopalakrishnan et al., 2021a). This model demonstrates a statistical error (MAPE) of less than 0.5% for predictions 1-4 weeks into the future. It was run at least weekly for more than a year to accurately predict ICU bed demand for Tampa General Hospital (Gopalakrishnan et al., 2021b). As input to the agent based simulation, the data from USAFacts was used to determine the initial probability that employees residing in a given county arrived at work in the infectious state. Since the worksite being modeled is in Santa Clara County, the transmission rate obtained from the epidemiological modeling of Santa Clara on any particular date was used in the agent simulation. This transmission rate varied over time, reflecting changes in local practices, behavior, and regulation (Gopalakrishnan et al., 2021b).

2.1.3 Model Calibration

The force of infection that drives new incidence in most epidemiological compartment models has the form

$$\beta SI/P \tag{1}$$

where S is the susceptible population, I the infectious population, P the total population, and β the transmission rate parameter (with typical units of 1/[*person-day*]). On the other hand, the disease transmission rate in a typical agent based model is stochastic and depends on the cumulative number of contacts between agents. Contact implies pairs of agents gathering within a hazard radius (defined as 6 feet in this model) with a smallest discrete time interval of 1.0 second. If two agents are within this defined radius for any period of time that is recorded as a hazard; but it is only a risk if one of the agents is infectious (shedding virus) and the other is susceptible. The total number of exposed agents (those becoming infected at work) depends on the cumulative contacts in [*person-seconds*]. This is not a universal number but depends on details of the workplace and agent behavior. To calibrate this stochastic transmission process, the cumulative number of hazardous encounters was measured for the simulated workforce with the building running at a normal capacity of 500 employees, and with no interventions in place. A single calibration parameter was then set so that the number of newly exposed agents (the incidence) matches that predicted for an equivalent population group in Santa Clara on the same date. This calibration factor was kept constant as other interventions and building policies were varied across multiple runs of the Agent Based Model.

2.2 Agent Based Modeling

In this section, we describe workplace modeling and interventions, creation of agents and their calendars, and our cloud-based simulation engine with user interface dashboard.

2.2.1 Building Structure and Locations

The workplace used for the agent based simulation was the IBM Almaden Research Center in San Jose, California. CAD drawings of the physical site were transformed into black and white bitmaps with a resolution of 0.454 [feet/pixel]. Fixed locations (pixels) representing destinations were assigned for all of-

fices, labs, bathrooms, auditorium and cafeteria entrances, conference rooms, and facilities sites, along with unique locations for all chairs in the cafeteria and auditorium. The building itself was divided into 12 partitions or tiles representing the different wings of the building at each floor. These partitions supported distribution of the simulation across multiple cloud compute nodes.

2.2.2 Path Finding

To determine the routes or paths agents would take during their daily activities in a simulation, a path finder leveraging a Bi-directional A* algorithm was employed. For each partition of the building, this path finder was used to generate all possible combinations of paths between each unique location. A path object is represented in our system as a structure with the following properties: identifier, starting and ending location, the owning partition, and a list of steps or coordinates comprising the path. These pre-computed paths were persisted in a database to be referenced by the simulation engine when constructing the plan needed by an agent to get from point A to B. While paths within partitions are pre-computed, paths across partitions were computed at run-time using breadth-first search across the connections defined in the building graph configuration, where nodes represent a partition and edges represent either stairs, elevators, or other way-points between partitions. Random selection of way-points was used to simulate agents making a decision about the choice of way-point they would use when crossing partition boundaries.

2.2.3 Employee Properties, Organization Chart, and Home Address

Synthetic employees were created programmatically, with a Poisson distribution on commute distance used to define employees' home addresses in nearby counties. An organizational chart was created with four levels of technical management up to and including the lab director (who reports to an offsite Director of Research). Facilities staff have a similar reporting structure under an offsite facilities director. Offsite agents were not explicitly modeled in the simulation. Each onsite employee and manager had a unique primary work location (e.g., office) and secondary work location (e.g., lab).

2.2.4 Employee Calendars

At the beginning of each workday, employee agents arriving at the site were each assigned a unique calendar of events with destination location and duration. These included work time intervals at primary and secondary work locations, coffee breaks (with a destination of the cafeteria), restroom breaks, meeting at a colleagues office, conferences, lunch breaks, and all hands meetings. Colleagues meetings were derived preferentially for using the org chart to favor meetings within an organization (including meetings between manager and employee). With all building paths pre-computed (see above), path IDs were associated with every employee calendar event based on the start and destination locations for the event. The calendar also included travel times to allow for transit of a given path (although traffic jams could result in a delayed arrival at a meeting or event).

2.2.5 Traffic Flow Model

Unobstructed, employees would move around the building following pre-computed paths with an initial velocity of 4.54 feet/second. People (like cars) can not move through one another. High densities are known to reduce speed - eventually leading to traffic jams. We based our model of walking speed on Newell's optimal velocity (OV) model (Newell, 1961; Wang et al., 2011), with velocity parameterised as a logistic function in density and described by the following equation:

$$s = \frac{1}{1+\exp^{k(n-n_0)}} \quad (2)$$

Where s is the scaling factor used for reducing walking speed, k is the logistic growth rate, n is the number of nearby agents, and n_0 is the midpoint. Values used for k and n_0 were 0.9 and 3.0 respectively. The number of nearby agents, n, is determined by superimposing a mesh with 1.8×1.8 ft^2 cells over the plan map, partitioning agents at each moment in time into velocity groups.

2.2.6 Interventions and Building Policies

Although the workplace modeled was calibrated for a typical occupancy of 500 employees onsite, the building occupancy does vary widely with, at times, over 700 employees (including summer interns), and of course many fewer onsite employees during the height of the pandemic. The number of onsite employees was varied (between 34-750) to study the effect of policy on disease hazard and risk. Two distinct methods were used to select this number for a given run: employees could be selected at random, or by third line organization in the org chart. In this way the org chart itself is used to model a particular social network graph. Another variable used in the simulation was the use (or non-use) of alternate entrances to densely populated areas including the auditorium

(one or two separate entrances), the cafeteria (one or three cash registers), etc.

2.2.7 Disease Transmission, Initialization, and Herd Immunity

At the start of each agent based simulation the initial infectious fraction is determined by public health prevalence data for the home counties of all employees on the date to be simulated. In the agent based simulation, a SEIR transmission process (Anderson and May, 1992) is used so that a *susceptible* individual in proximity to an *infectious* individual has the potential to move the *susceptible* individual to an *exposed* state. In the *exposed* state individuals are incubating the virus but not yet infectious. The incubation period is chosen as one day, so that individuals *exposed* at work return in the infectious state the next day.

To understand how vaccination and recovery from prior infection is handled, first consider that in epidemiological compartment modeling, recovered and vaccinated individuals are often referred to as *removed*, or in one or more *R* compartments. This is the case because the force of infection depends only on the fraction of individuals *susceptible*, *S*, and the fraction *infectious*, *I*. Over time, waning immunity may lead to removed individuals returning to a susceptible state, but instantaneously they are not part of the force of infection. This is also reflected in the definition of the effective reproductive number (R_t) which is a re-scaling of the basic reproductive number (R_o) by the fraction of susceptible individuals. i.e.,

$$R_t \sim R_0(S/N),$$

where N is the total agent population. We take advantage of this fact in our experimental design by initializing the simulation beginning with all employees either in a *susceptible* or *infectious* state, and generating multiple runs *as a function of* onsite employee population. In so doing the results can be applied to *any* level of initial herd immunity simply by re-scaling the building population by the fractions susceptible. For example, in a building with population of 1001 individuals (one infectious), if 50% are initially immune (removed) due to previous infection or from vaccinations, then the outcome of the simulation is mathematically identical to a simulation run with 500 susceptible individuals (and a single infectious). Accordingly, estimation of the removed population for any simulation date can be performed as a post processing step and the appropriately re-scaled population used to predict hazard and risk on that date. This approach will be explained in detail in the *results and discussion* section 3.

2.2.8 Batch Runs

To examine a policy choice, one would like to run a batch of agent simulations over a matrix of configuration parameter values, saving recorded hazards and risks as a function of the parameter matrix. When the batch run of simulations is complete, we would tend to favor a policy choice that minimizes the estimated hazards and risks. Ideally, there is a base level of acceptability when the risk from working at the workplace is approximately equal to the risk of working at home over the same 8 hour work window.

We have built a batch run system to examine policy choices, where the batch run is specified by a set of configuration parameters to vary, plus the set of possible values. The batch system forms the outer product of the parameter choices; for N parameters, we form a N-D tensor of all the parameter combinations. After forming the tensor, the batch system calls the main simulation engine for each tensor cell, recording the resulting hazards and risks in an event database. Graphs and data analysis is performed by rolling up results across parameter values.

2.2.9 Cloud Architecture

Fig. 1 shows our agent based simulation engine as deployed on Red Hat OpenShift v4.6 in the IBM Cloud. RedHat OpenShift is a platform as a service based on Kubernetes (Vayghan et al., 2018) providing software developers tools for creating and managing cloud native applications using Linux containerization technologies. Our cloud instance is comprised of 6 compute nodes, with each node having 16 CPUs (Intel Xeon CPU E5-2683 @ 2.00GHz) and 64 GB RAM.

The data for simulations, which included details such as agent properties, building locations, disease states, events, paths, etc. were stored as JSON documents in CouchDB (Manyam et al., 2012). The database instances were configured in cluster mode, having three replicas for high availability, and with replication between instances enabled for redundancy.

Microservices providing Application Programming Interfaces (APIs) in support of various functions such as retrieving and modification of data contained within the CouchDB instances were developed with LoopBack v4. LoopBack is an open-source framework based on Node.js, Typescript, and OpenAPI standards enabling developers to build APIs for accessing database backends and other web based services quickly. Additionally, we deployed an API gateway based on aiohttp and Python 3.9 to provide a consolidated interface to the microservice APIs deployed in our cluster.

The simulation engine was deployed as a set of

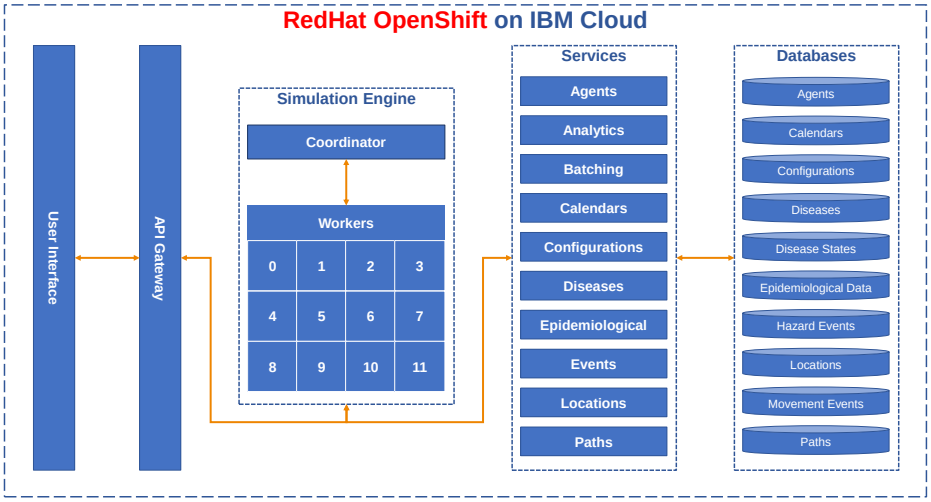

Figure 1: Agent based simulation engine deployed on RedHat OpenShift in the IBM Cloud.

containerized processes representing a coordinator and a set of workers. These individual components were developed with Python 3.9.9 using the aiohttp package as the basis for the communication model. The coordinator is responsible for keeping the simulation date and time, controlling synchronization, and reconciling the entering and exiting of agents between workers. A worker process is deployed for each part of the building or partition it represents. For our simulation of the IBM Almaden Research Center, we divided the building into 12 distinct partitions. To simulate an alternative site would simply require deploying fewer or additional worker processes depending on the layout of the building. Workers are responsible for computing their part of the simulation, which includes steps such as handling new calendar events, moving agents within and between partitions, proximity detection, and disease transmission. These processes would utilize the microservices mentioned previously to create and update simulation data such as movement and hazard events and disease states for the agents.

As mentioned previously, the coordinator controls the overall flow of the simulation. Its primary job is to handle the synchronization of a tick of the clock. A tick in our simulations is defined as 5 seconds. Thus, every call the coordinator makes to the workers to progress will represent 5 seconds of elapsed time in the simulated world. Furthermore, workers will perform a micro-tick analysis at 1 second intervals within the 5 second tick for analyzing the movement, proximity, and disease transmission of agents. This fine-grained timing allows our system to record very detailed information regarding the progress of a simulation.

Analytics based on the outcome of the simulations can be queried and viewed as plotted images and JSON output. The JSON output provides users the capability to use the summarized results in their own analytic or graphing tools. CouchDB views were employed to transform the raw movement, hazard, and agent disease state data into summarized results after a completed work day. Fig. 2 shows an example heatmap visualization of agent-to-agent exposures (red) in one simulated day in the cafeteria dining area of Almaden Research Center, outlined in dark blue. Through this service an operations officer has the tools at hand to make data driven decisions and apply policy actions depending on the outcomes.

Figure 2: Example heat map of COVID-19 exposures (red) in one partition of Almaden Research Center, showing most simulated exposures happen in the cafeteria dining area (outlined in blue).

2.2.10 User Interface

To visualize the simulations, we developed a web-based application based on React v17.0.2 and de-

ployed in our OpenShift cluster along with our other components and microservices. Fig. 3 shows an example of our web application with the 2nd floor, D-wing as the focus. The application provides the ability to see the entire layout of a building and view the instantaneous locations of the agents. Depending on their disease state, agents will either appear in one of the possible 4 colors: blue for *susceptible*, red for *infected*, yellow for *exposed*, and green for *recovered* or *vaccinated*. The application provides users the ability to select the date and time period, as well as the playback speed of a simulation. Our application also provides additional filtering capabilities for viewing agents of selected states, selecting agents by their serial number, and recorded exposures. Lastly, the web application is integrated with our API gateway and analytic services providing users a single purpose application for working with simulations.

3 RESULTS AND DISCUSSION

From the data generated by the agent based simulation it is possible to measure both the hazard and the risk associated with transmission of the SARS-CoV-2 virus. Hazard reflects the frequency and duration of encounters between people within a configurable hazard radius (6 feet in these simulations). It does not depend upon - or presuppose - disease transmission. Transmission risk exists only when both susceptible and infectious individuals are in the building. We note that other hazardous factors could be modeled, and studied, but in the case of aerosol transmission of an infectious disease the proximity of people to one another is fundamental to the hazard - and to any interventions designed to remediate it.

3.1 Hazard Distribution

Figs. 4a-4d show the distribution of hazard exposure as a function of number of employees in the building. As defined previously in section 2, the units of hazard are [person-seconds]. The data is shown as a series of violin plots, where each sub-figure represents the outcome from a different run condition. In Fig. 4a, on site employees are selected by third line organization and alternate routes are disabled, while in Fig. 4b, on site employees are selected by third line organization and alternate routes are *enabled*. In Fig. 4c, on site employees are selected at random and alternate routes are disabled, and in Fig. 4d, on site employees are selected at random and alternate routes are *enabled*. Each violin represents one full day run of the simulation using five different random number seeds. In all cases the daily hazard exposure increases systematically with building occupancy.

The total work force hazard based on person-person contact time is shown in Fig. 5. The units are *[person-seconds]*. The standard deviation is obtained by averaging the mean hazard for each distribution over the five trials. For those run conditions where the employee population is selected at random, the number of employees selected is exact and plotted along the abscissa. Where on-site employees are selected by the number of third line management organizations allowed in the building, the number of employees will vary with randomized trial as third line organizations vary in size. This variation is shown as a horizontal error bar for this mode of population selection. To understand the vertical scale in Fig. 5, if the workforce hazard is (for example) 150,000 [person-secs]) with 500 employees in the building, that corresponds to an average person-person exposure of 300 person-seconds of contact per employee over the 8 hour day. Note that the measured hazard does not always follow a simple linear relation with building occupancy. In particular, for occupancy determined by selecting third line organization(s), and with alternate routes enabled, the measured hazard follows the hazard vs number of employees for selection by third line organization(s), and without alternate routes, until a building population of 300 employees where there is a knee in the data and hazard increases at a reduced rate for alternate routes enabled (orange symbols).

In all cases the mean hazard-exposure increases with building occupancy. Selecting employees by third line organization leads to systematically higher hazard than random selection. Supporting alternate routes to reduce crowding systematically lowers hazard exposure. The observed variation with run conditions demonstrates that the occupational hazard depends both on the the physical layout of the building as well as the social (or organizational) network graph reflecting connections between people. Either can be effectively modified by appropriate interventions and the corresponding outcomes can be measured. Observe that for each run condition, the hazard data was fit with a linear least squares fit with respect to the number of employees, but in general the observed hazard vs number of employees on-site may not always be linear. This is particularly evident for the runs where on-site employees were selected by organization, and alternate routes were allowed. Alternate routes are most effective in reducing hazard when and if crowded conditions such as extended cafeteria checkout lines are a significant source of person-person contact. This crowding is and of itself nonlinear, and the non-linearity is observed for

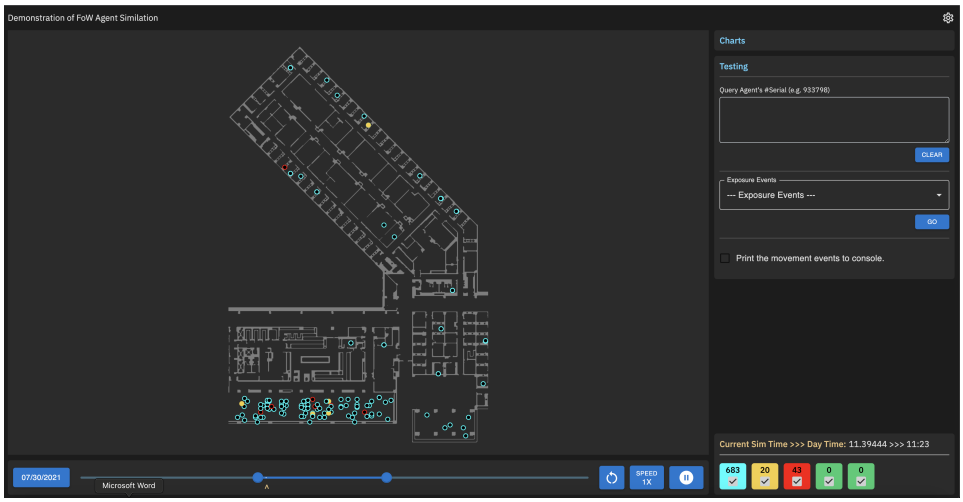

Figure 3: User interface for the agent based simulation engine showing a zoomed in view of a running simulation for the 2nd floor D-wing of the building during lunch time.

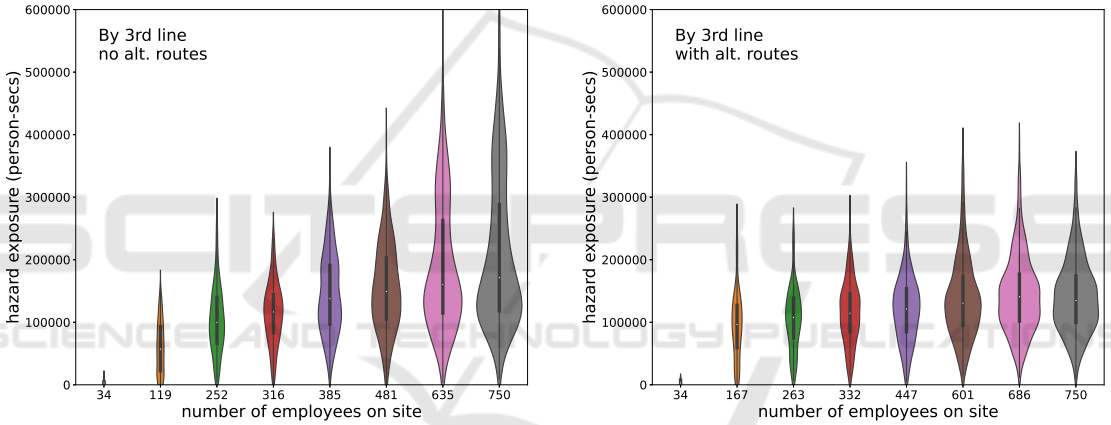

(a) Employees selected by org, alt. routes disabled

(b) Employees selected by org, alt. routes enabled

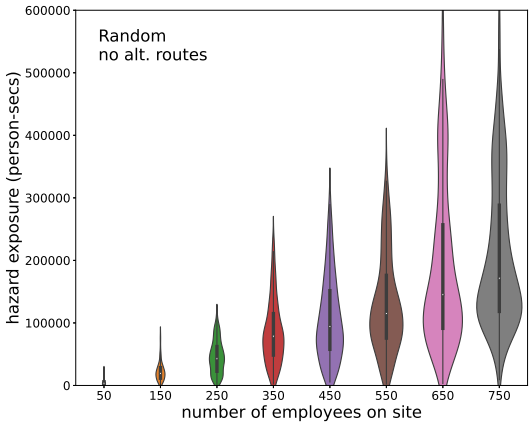

(c) Employees selected at random, alt. routes disabled

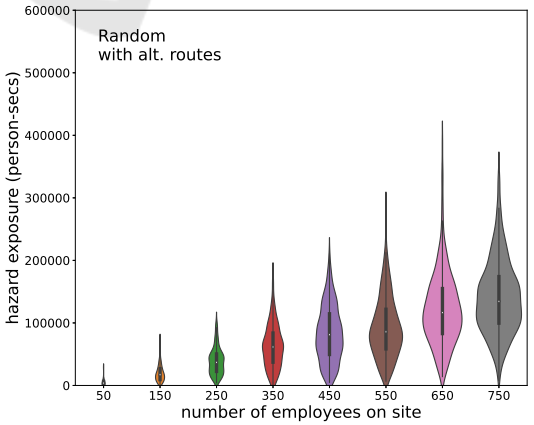

(d) Employees selected at random, alt. routes enabled

Figure 4: Violin plots showing the hazard exposure [person-seconds] distribution as a function of the number of onsite employees. Each sub-panel corresponds to a different run condition. For all run conditions the average daily hazard increases with building occupancy.

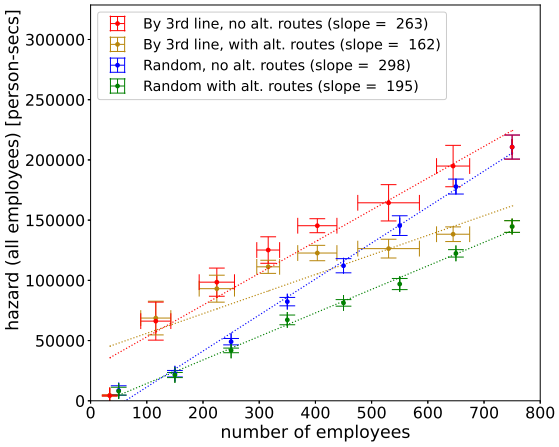

Figure 5: The figure shows the total work force hazard (person-person contact time [person-seconds]) as a function of the number of onsite employees. The data was obtained by averaging the mean hazard (see Figs. 4a-4d) over five runs with different random number seeds. In all cases the employee-employee contact time increases with building occupancy. Selecting employees by third line organization leads to systematically higher hazard than random selection. Supporting alternate routes to reduce crowding systematically lowers hazard exposure.

relatively high building populations. This is to be expected given the non-linearity of traffic flow (and of Newell's optimal velocity model used in this simulation (Newell, 1961; Wang et al., 2011)).

3.2 Risk of Disease Transmission

Figs. 6a-6d show the number of employees infected as a function of time since midnight [hours] for four run conditions. When infected, susceptible employees first enter a latent *exposed* state, and become *infectious* on the following day. The number of employees on site is selected by organization, or selected at random; each with and without the use of alternate routes. Each sub-figure shows a series of runs with varying average number of employees on site (shown in the legend). Each curve represents an average over five runs with five random number seeds. The standard deviation is shown at the end of each workday. In all cases, for all runs, the run duration was a one full business day. The curves represent the average cumulative sum of infections over the day. Each curve terminates at a slightly different time based on the time of the *final* infection for that run condition.

Based on individual calendars, arrival times for employees varies between 6:30am and 10am. The rate of new infections (the slopes in Figs. 6a-6d) starts at zero at 6:30am when the building is empty, reaches a maximum around lunchtime where the largest groups gather in the cafeteria, and falls off again as people leave at the end of the day. Disease transmission is a stochastic process and the number of individuals exposed at work (and the time of day for the exposures) varies from run to run. The dashed lines represent the number of *expected* infections had a sub-population of the same size remained at home.

Based on the cumulative disease exposures during the workday, Fig. 7 shows the infection *risk* vs. the number of employees in the building. The infection risk is measured by the cumulative number of newly infected (exposed) employees over the full workday. The total risk is measured in five trials for the run conditions shown in the legend. Once again, where on-site employees are selected by third line organizations, the number of employees varies with randomized trial. This variation is shown as a horizontal error bar for this mode of population selection. For each of the run parameters (or mode) listed in the legend, we also show the slope based on a least squares fit to the data. This slope represents the incremental increase in infection risk as additional employees arrive in the building.

In Fig. 7, in black, we plot the *expected* number of new exposures for the same sub-population if the individuals remained in their home counties and not come to work. This is derived from the county level SARS-CoV-2 epidemiological modeling and prevalence data scaled to the same sub-population size.

As discussed above, none of the results from the agent based simulation are universal, since they are a function of both building layout, workplace policies, and other interventions including the size of the onsite workforce. However, for any particular workplace or model workplace, it is possible to quantitatively compare the on-site risk to the corresponding risk if the same sub-population of employees were to remain at home. In Table 1 we list, for each mode, the incremental increase in risk as a function of the number of onsite employees (the slope in Fig. 7), as well as the number of onsite employees at which the total onsite risk is equivalent to the current at home risk. This is the point at which the risk lines for on-site employees crosses the average risk line for the same sub-population at home. As is the case in Fig. 7, the population size along the x-axis does not include individuals in an immune or *removed* state, so if the risk lines cross, the onsite population can be re-scaled. For example, at 100 employees, and if 50% of employees are known to be fully vaccinated or otherwise immune, then the risks become equivalent for 200 on site employees. This crossing point does not represent zero risk, it simply identifies the onsite population and policies, for a particular workplace site, where the average occupational risk would most closely match the

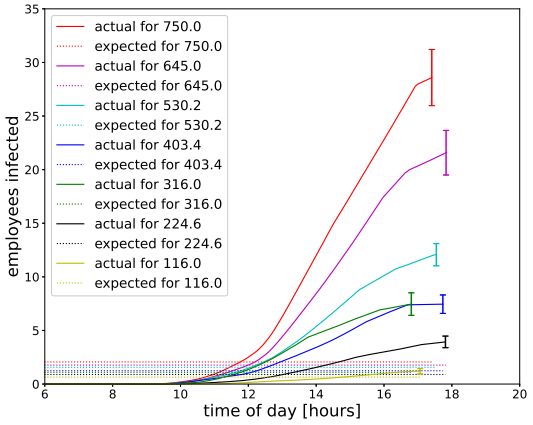

(a) Employees selected by org, alt. routes disabled

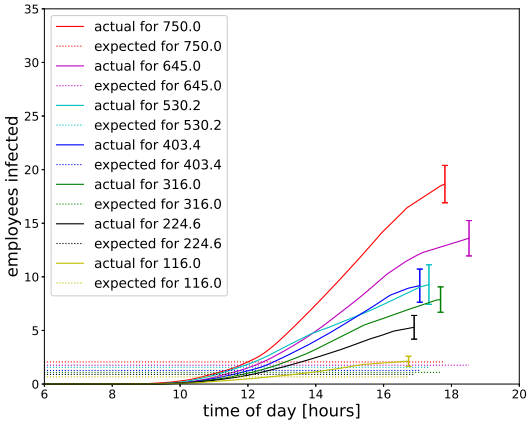

(b) Employees selected by org, alt. routes enabled

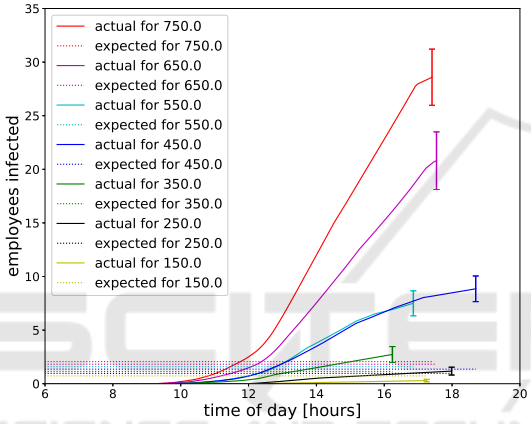

(c) Employees selected at random, alt. routes disabled

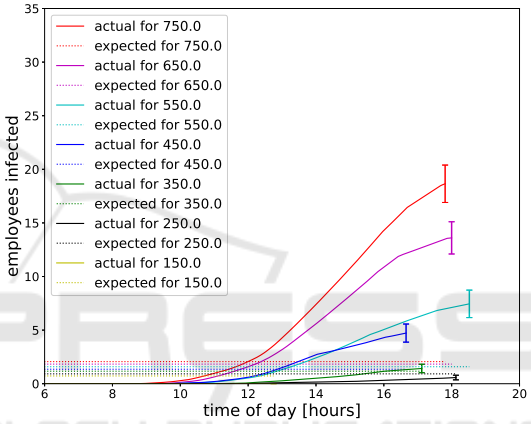

(d) Employees selected at random, alt. routes enabled

Figure 6: Number of employees infected as a function of time of day [hours], and as a function of number of employees on site, for four run conditions with on site employees selected by organization or at random, with and without the use of alternate routes. Each subfigure shows the average number of onsite employees (averaging over 5 random trials, with std. dev. shown at the end of each workday). The dashed lines represent the total number of *expected* infections during the eight hour workday had a sub-population of the same size remained at home.

average at home risk. Defining an *acceptable* occupational risk is, of course, a matter of policy. A zero risk criteria would never support even partial return to work policy. One might choose an intermediate policy such that *acceptable* occupational risk should, on average, be half the current at home risk. Modeling can not select criteria, but given the criteria, modeling can evaluate the interventions and policies required to achieve the defined goal.

To examine using the intersection of risk lines as a policy recommendation to a workplace site manager, we performed a historical analysis of our simulation system, looking at how the crossover point moved over nine months of the COVID-19 pandemic from July, 2021 to March, 2022. For each date, we ran 25 simulations (5 capacities $\times$ 5 random seeds) to produce a risk vs. number employees chart such as

Table 1: The incremental risk per person working onsite (from Fig. 7) and the estimated building occupancy where total onsite risk is equivalent to the current at home risk for each mode or site policy.

Mode	**Incr. risk per person**	**Bldg. Occ. (+/- 5)**
Random, with alt. routes	0.022	178
Random, no alt. routes	0.035	172
By 3rd line, with alt. routes	0.019	0
By 3rd line, no alt. routes	0.032	85

Fig. 7. Following the lowest risk policy choice from our prior analysis, the simulations reduce agent populations randomly and alternate routes are enabled, so we are focused on risk vs. number employees at each date. For each chart, we estimated the best fit lines

Table 2: Historical analysis of crossover capacity during the Delta and Omicron waves. For nine dates from July, 2021 through March, 2022, we repeated the risk crossover analysis of Fig. 7 to estimate the recommended site capacity at IBM Almaden Research Center. The recommended site capacity is lowest at the peaks of the Delta and Omicron COVID-19 peaks, highlighted in red and blue.

	Date (10th of each month)								
	2021						**2022**		
	Delta						Omicron		
	Jul	Aug	Sep	Oct	Nov	Dec	Jan	Feb	Mar
Crossover Capacity	155	142	157	180	168	177	130	154	157

to: 1) estimated risk, and 2) expected risk, and we found the intersection point where the risk levels cross one another, which can be taken as a recommended workplace site capacity. In Table 2, we show the recommended capacities for these nine dates, the 10th of the month from July, 2021 through March, 2022, which includes both the Delta and Omicron COVID-19 peaks in the US (highlighted as red and blue in Table 2). As we were hoping to see, the recommended capacity drops to its lowest points at the peaks of the Delta and Omicron waves.

4 CONCLUSION

To advise workplace site managers on handling hazard and risks from infectious diseases such as COVID-19, ideally one would like to explore the effects of different policies using a data-driven approach. Agent simulation provides a lens for exploring policy choices by systematically altering simulation parameters. The differing simulation parameters changes the physical interactions between virtual employees traversing a virtual workplace, yielding different levels of hazard and risk. In a simulation of a large research laboratory with maximum capacity of 750, we compared the effects of reducing the population by randomly selecting employees in the organization chart with eliminating some number of third line organizations. We also explored simulations with and without the benefits of alternate routes available to the agents for social distancing (e.g. multiple cash registers, multiple auditorium entrances). Comparing the hazards and risks from these options, we showed that the random selection method was the best, and that alternate routes do result in lower virus transmission. For the various parameter choices, we can plot hazard and risk for different levels of building occupancy, and we estimate the number of employees who can "safely" work in the building. Here, "safe" is the point where workplace virus risk is the same as working at home, which is estimated by county epidemiological modeling. Even if one wants to operate at a stricter level of safety, the agent simulation framework is general enough to provide valuable guidance to a workplace site manager.

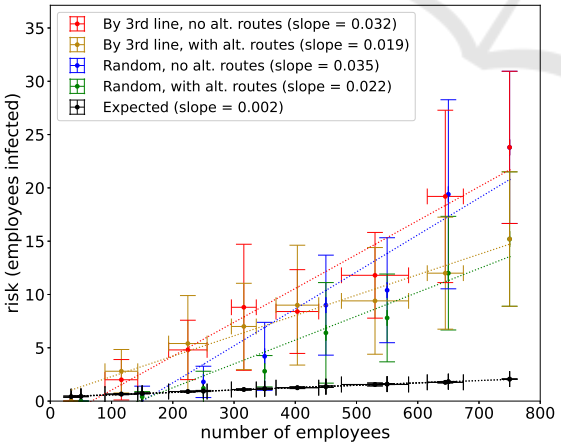

Figure 7: The figure shows the infection risk as measured by the cumulative number of infected employees over one workday as a function of the number of employees in the building. The error bars reflect the standard deviation over five trials with different random number seeds. Each line represents a different set of run conditions as indicated in the legend. The black data show the expected number of new infections (based on the county level epidemiological data) had the same sub-population stayed at home.

REFERENCES

Alamoudi, E., Mehmood, R., Aljudaibi, W., Albeshri, A., and Hasan, S. H. (2020). Open Source and Open Data Licenses in the Smart Infrastructure Era: Review and License Selection Frameworks. In *Smart Infrastructure and Applications*, pages 537–559. Springer.

Anderson, R. M. and May, R. M. (1992). *Infectious Diseases of Humans: Dynamics and Control*. Oxford University Press.

Baldassi, F., D'Amico, F., Malizia, A., and Gaudio, P. (2021). Evaluation of the Spatiotemporal Epidemiological Modeler (STEM) during the recent COVID-19 pandemic. *The European Physical Journal Plus*, 136:1072.

Bianco, S., Capponi, S., and Kaufman, J. H. (2021). Matematica epidemiologica per COVID-19. *Ithaca: Viaggio nella Scienza*, 2021(17b):5–12.

Bourgais, M., Taillandier, P., and Vercounter, L. (2019). BEN: An Agent Architecture for Explainable and Expressive Behavior in Social Simulation. In *EXTRAAMAS*, Montreal, Canada.

Chang, S., Pierson, E., Koh, P. W., Gerardin, J., Redbird, B., Grusky, D., and Leskovec, J. (2021). Mobility network models of COVID-19 explain inequities and inform reopening. *Nature*, 589:82–87.

Chang, S. L., Harding, N., Zachreson, C., Cliff, O. M., and Prokopenko, M. (2020). Modelling transmission and control of the COVID-19 pandemic in Australia. *Nature Communications*, 11(5710).

Daniels, R., Gilbert, S., Kuppusamy, S., Kuempel, E., Park, R., Pandalai, S., Smith, R., Wheeler, M., Whittaker, C., and Schulte, P. (2020). Current Intelligence Bulletin 69: NIOSH Practices in Occupational Risk Assessment. *National Institute for Occupational Safety and Health*.

Douglas, J. V., Bianco, S., Edlund, S., Engelhardt, T., Filter, M., Günther, T., Hu, K., Nixon, E. J., Sevilla, N. L., Swaid, A., et al. (2019). STEM: an open source tool for disease modeling. *Health security*, 17(4):291–306.

Duggirala, M., Singh, M., Hayatnagarkar, H., Patel, S., and Balaraman, V. (2016). Understanding impact of stress on workplace outcomes using an agent based simulation. In *Proceedings of the Summer Computer Simulation Conference*, pages 1–10, Montreal, Canada.

Edlund, S. B., Davis, M. A., and Kaufman, J. H. (2010). The spatiotemporal epidemiological modeler. In *Proceedings of the 1st ACM International Health Informatics Symposium*, pages 817–820.

Gopalakrishnan, V., Navalekar, S., Ding, P., Hooley, R., Miller, J., Srinivasan, R., Deshpande, A., Liu, X., Bianco, S., and Kaufman, J. H. (2021a). Adaptive Epidemic Forecasting and Community Risk Evaluation of COVID-19. *arXiv preprint arXiv:2106.02094*.

Gopalakrishnan, V., Pethe, S., Kefayati, S., Srinivasan, R., Hake, P., Deshpande, A., Liu, X., Hoang, E., Davila, M., Bianco, S., et al. (2021b). Globally local: Hyperlocal modeling for accurate forecast of COVID-19. *Epidemics*, 37:100510.

Hardy, P., Marcolino, L. S., and Fontanari, J. F. (2021). The paradox of productivity during quarantine: An agent-based simulation. *The European Physical Journal B*, 94(1):40.

Hinch, R., Probert, W. J. M., Nurtay, A., et al. (2021). OpenABM-Covid19 — An agent-based model for non-pharmaceutical interventions against COVID-19 including contact tracing. *PLOS Computational Biology*, 17(7):1–26.

Hosseini, P. R., Mills, J. N., Prieur-Richard, A.-H., et al. (2017). Does the impact of biodiversity differ between emerging and endemic pathogens? The need to separate the concepts of hazard and risk. *Philosophical Transactions of the Royal Society B: Biological Sciences*, 372:20160129.

Islam, M. T., Jain, S., Chen, Y., et al. (2022). An Agent-Based Simulation Model to Evaluate Contacts, Layout, and Policies in Entrance, Exit, and Seating in Indoor Activities Under a Pandemic Situation. *IEEE Transactions on Automation Science and Engineering*, 19(2):603–619.

Kaufman, James H., e. a. (2006-2022). The Eclipse SpatioTemporal Epidemiological Modeler (STEM) website. https://projects.eclipse.org/projects/technology.stem/.

Kerr, C. C., Stuart, R. M., Mistry, D., et al. (2021). Covasim: An agent-based model of COVID-19 dynamics and interventions. *PLOS Computational Biology*, 17(7):1–32.

Kumpulainen, S. (2006). Vulnerability concepts in hazard and risk assessment. In Schmidt-Thome, P., editor, *Natural and Technological Hazards and Risks Affecting the Spatial Development of European Regions*, Special Paper 42, pages 65–74. Geological Survey of Finland.

Manyam, G., Payton, M. A., Roth, J. A., Abruzzo, L. V., and Coombes, K. R. (2012). Relax with CouchDB — Into the non-relational DBMS era of bioinformatics. *Genomics*, 100(1):1–7.

Muñoz, S. and Iglesias, C. A. (2021). An agent based simulation system for analyzing stress regulation policies at the workplace. *Journal of Computational Science*, 51:101326.

Newell, G. F. (1961). Nonlinear effects in the dynamics of car following. *Operations research*, 9(2):209–229.

Sage, A. P. and White, E. B. (1980). Methodologies for risk and hazard assessment: A survey and status report. *IEEE Transactions on Systems, Man, and Cybernetics*, 10(8):425–446.

Shattock, A. J., Le Rutte, E. A., Dünner, R. P., Sen, S., Kelly, S. L., Chitnis, N., and Penny, M. A. (2022). Impact of vaccination and non-pharmaceutical interventions on SARS-CoV-2 dynamics in Switzerland. *Epidemics*, 38:100535.

Taillandier, P., Gaudou, B., Grignard, A., et al. (2018). Building, composing and experimenting complex spatial models with the GAMA platform. *GeoInformatica*, 23:299–322.

USAFacts (2020). US Coronavirus Cases and Deaths. https://usafacts.org/visualizations/coronavirus-covid-19-spread-map. Accessed: 2020-10-04.

Vayghan, L. A., Saied, M. A., Toeroe, M., and Khendek, F. (2018). Deploying Microservice Based Applications with Kubernetes: Experiments and Lessons Learned. In *2018 IEEE 11th international conference on cloud computing (CLOUD)*, pages 970–973. IEEE.

Vitins, B. J., Erath, A., and Axhausen, K. W. (2016). Integration of a Capacity-Constrained Workplace Choice Model: Recent Developments and Applications with an Agent-Based Simulation in Singapore. *Transportation Research Record*, 2564(1):1–13.

Wang, H., Wang, W., and Chen, J. (2011). General Newell model and related second-order expressions. *Transportation Research Record*, 2260(1):42–49.